UCRL-JC-131591
Preprint

An Electromagnetic Induction Tomography Field Experiment at Lost Hills, CA

H. M. Buettner and J. G. Berryman

This paper was prepared for submittal to
Symposium of the Application of Geophysics to
Engineering and Environmental Problems
(SAGEEP)
Oakland Marriott Center, Oakland, CA
March 14-18, 1999

November 3, 1998

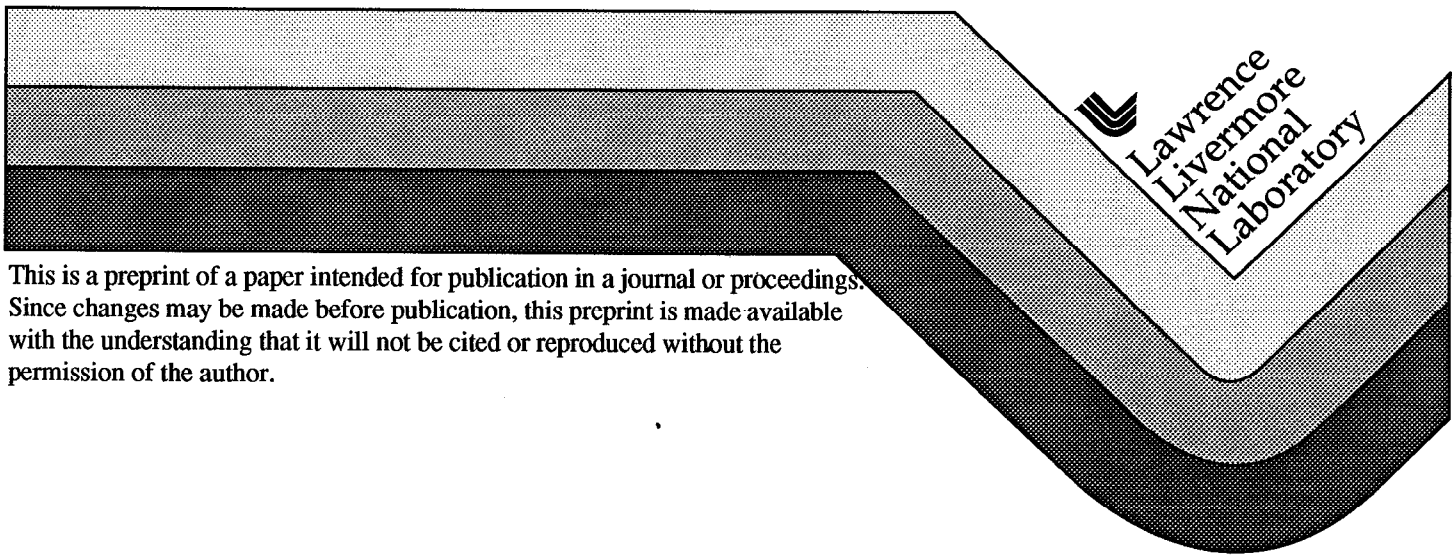

An Electromagnetic Induction Tomography Field Experiment at Lost Hills, CA

H. Michael Buettner and James G. Berryman
Lawrence Livermore National Laboratory
P. O. Box 808, Livermore, CA 94551-9900

Abstract

We have collected borehole to surface electromagnetic induction field data for a shallow steam injection that is underway at Mobil Oil's Lost Hills-3 field in San Joaquin Valley. Earlier work had been done at the same site by Wilt *et al.* (1996). This site is an interesting test for techniques under development for environmental engineering, because it can be viewed as an excellent analog of a shallow environmental remediation using steam injection. Surface magnetic field data (vertical and radial fields, magnitude and phase) were collected using 18 receiver stations along two profiles which ran radially from the EM transmitter well from 5 m to 120 m. The data at each surface station were collected while the EM transmitter was raised slowly from a depth of 120 m to a final depth of 20 m. As part of this experiment, a calibration of the EM transmitter was also performed. Magnetic field data from Lost Hills were successfully collected, including both vertical and horizontal (surface radial) magnitude and phase data along a northerly profile and along a westerly profile. We have observed that the radial receiver data appear to be better behaved than the vertical receiver data, suggesting that these data may be less sensitive to environmental clutter (numerous metallic pipes crisscrossing the site at the surface) than are the vertical data. Some simple 1-D modeling has been done to confirm that the expected conductivity change in the steam zone should produce an observable anomaly in the measured data when comparing the pre-steam to the post-steam conditions. Results of this test were positive. Further analyses of these data making use of a new code developed in a companion paper are in progress and will presented separately.

1 Introduction

Electromagnetic induction tomography is a promising new tool for imaging electrical conductivity variations in the earth (Wilt *et al.*, 1995a,b). The source field is a magnetic field generated by currents in wire coils. This source field is normally produced in one borehole, while the received signals are the measured small changes in magnetic field in another, more distant borehole; however, the method may also be used successfully in combination with surface sources and receivers. The goal of this procedure is to image electrical conductivity variations in the earth, much as x-ray tomography is used to image density variations through cross-sections of the body. Although field techniques have been developed and applied previously to collection of such EM data, the algorithms for inverting the magnetic field data to produce the desired images of electrical conductivity have not kept pace. The current state of the art in electromagnetic data inversion (Alumbaugh and Morrison, 1995a,b) is based on the Born/Rytov

approximation (requiring a low contrast assumption), even though it is known that conductivity variations range over several orders of magnitude and therefore require nonlinear analysis. The goal of our work is therefore to join theory and experiment to produce enhanced images of electrically conducting fluids underground, allowing better localization of contaminants and improved planning strategies for the subsequent remediation efforts.

Electromagnetic induction logging has long been used in the petroleum and environmental industry to measure the electrical conductivity in the region immediately surrounding the borehole. This data, which is used to estimate pore fluid saturations near the well, is very sensitive to variations in rock pore fluid. Mapping surface variation of conductivity has also been found to be a very sensitive indicator of zones of higher salinity and acidity in many shallow environmental studies.

Recent research at LLNL (Newmark and Wilt, 1992; Wilt and Schenkel, 1992; Tseng *et al.*, 1995; Berryman, 1997; 1998) has developed instrumentation and software to deploy EM induction technology in crosshole and surface-to-borehole configurations, thereby extending the conductivity information to the region between boreholes. The result is a determination of subsurface conductivity at a much higher resolution than can be achieved with surface techniques and much greater penetration than can be achieved with radar technology.

Although other technologies, such as ERT (Berryman and Kohn, 1990; Daily *et al.*, 1992; Ramirez *et al.*, 1993; Borcea, 1996; Borcea *et al.*, 1996), can produce electrical conductivity images at a useful spatial scale, the advantage of the electromagnetic induction technology (EMIT) is that we can make use of existing monitoring wells and the surface to do imaging. Since signals are transmitted and received inductively, we do not need to make ground contact (no ground penetrating electrodes); the technology is therefore relatively noninvasive. Furthermore, all conductors present can in principle be imaged using the EMIT technique, whereas ERT can only image those conductors maintaining a continuous electrical current path with the source and/or receiver electrodes. There is also the important potential advantage that multiple frequencies can be employed to improve the imaging capability for electromagnetic induction tomography; this feature is simply not available with ERT imaging since the inversion methods used to date are inherently based on the DC (zero frequency) limit of the pertinent equations.

We have had good success deploying the EM induction technology in petroleum applications for field characterization and steam flood monitoring, but it has yet to be used in noisy urban areas where we are often unable to drill holes or do anything invasive. The targets for imaging in environmental problems are significantly more variable than in the petroleum production environment, ranging from highly resistive DNAPLs and petroleum products to highly conducting acidic brines.

In this paper, we describe the results of a field test of EM induction conducted at an oil field site near Lost Hills, CA. The shallow steam flood being conducted at this site can be thought of as an analog of an environmental cleanup operation.

2 The Site

At the Lost Hills site, steam has been injected into upper, middle, and lower zones of the Tulare formation since 1991 using injector 5035 as shown in Figure 1. More recently injector 5035 was refractured with steam, and service well O35 was completed as an injector for the middle and lower zones in order to increase the injection rate. The object of our monitoring was the shallow

zone which extends from about 60 m to 85 m depth. Further details about this site and other EM work performed there can be found in a report by Wilt *et al.* (1996).

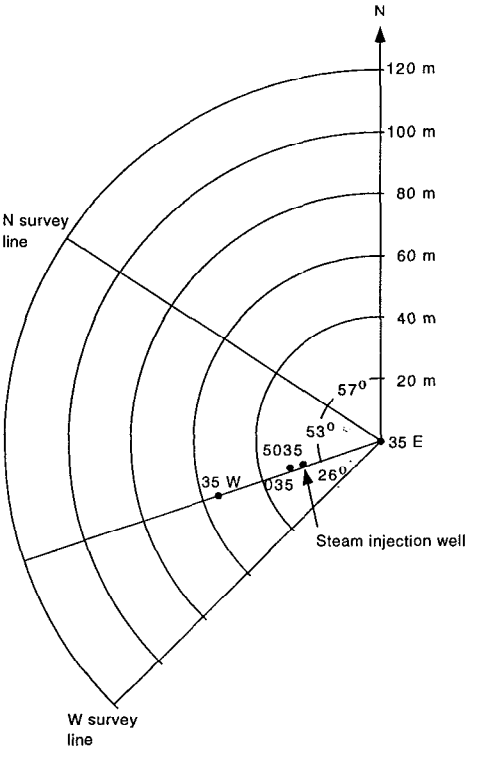

Figure 1: Plan view of the survey lines and well locations.

3 The Experiment

A plan view of the well locations and survey lines is also shown in Figure 1. Our EM transmitter was located in well 35E, and operated between depths of 20 m and 120 m. It produces a vertical magnetic moment, *i.e.*, a vertical magnetic dipole. Our receiver coils were moved out along the North and West survey lines at regular intervals for data collection. The distances from 35E were 5, 10 15, 20, 25, 30, 35, 40, 45, 50, 55, 60, 70, 80, 90, 100, 110, and 120 m along each of the survey lines. Both vertical and radial components of the magnetic field were measured. Well 35W was used for cross borehole imaging in the earlier work of Wilt *et al.* (1996), but was not used in this work.

A schematic diagram of the measurement system is show in Figure 2. The electronics portion consists of 1) a signal source operating at a constant frequency (1220 Hz) which feeds a power amplifier to drive the downhole transmitter coil, 2) four receiver coils connected via coaxial cables to four lock-in amplifier detectors for measuring signal magnitude and phase, 3) a reference signal (optically isolated) derived from the transmitter excitation signal which is

fed to the lock-in detectors as their phase reference, and 4) a laptop computer which controls the movement of the transmitter coil in well 35E and which records the data. The mechanical portion of the system consists of a boom truck which is used to raise and lower the transmitter coil in well 35E, and a shaft encoder which provides depth information.

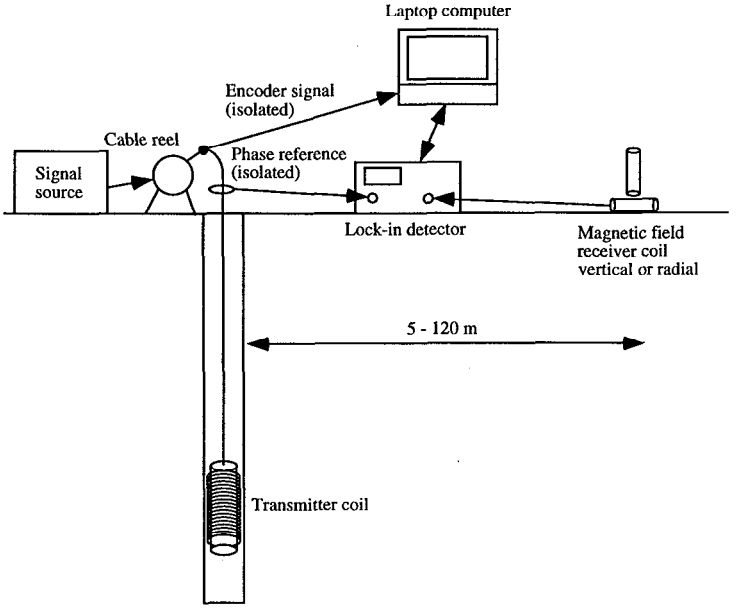

Figure 2: Schematic diagram of EM measurement system.

4 Results

Data were collected along the North and West survey lines at regular intervals as described above. The data were collected in the following manner. The transmitter coil was lowered to the bottom of its run at a depth of 120 m, and the four receiver coils were laid out in plastic-lined, shallow, vertical holes to measure the vertical component of the magnetic fields at 5, 10, 15, and 20 m along the North survey line. The vertical magnetic fields were then measured and recorded as the transmitter coil was slowly raised to a depth of 20 m. Next the coils were taken out of their plastic-lined holes, laid out on the ground surface at 5, 10, 15, and 20 m and oriented radially for collecting the radial magnetic fields. The radial fields were measured and recorded as the transmitter coil was slowly raised from 120 m to 20 m. The set of four coils was then moved to 25, 30, 35, and 40 m, and the process repeated until the North survey was completed. The same procedure was then used for data acquisition in the West survey.

After all of the data were collected, a total system calibration was performed for reducing the data. Throughout the calibration procedure, the system was configured exactly as it was while collecting the data. That is, all the components were connected in the same way with the same cables. The calibration consisted of three parts: First, the four coils were calibrated relative to each other. To do this, the coils were placed near each other, and at the same

distance from the transmitter well with all coils oriented radially. The transmitter coil was excited at the same frequency and current drive level that was used to collect the data. The received signals (magnitude and phase) were measured in all four coils. Since all four receiver coils saw the same magnetic field, they could now be calibrated relative to each other.

Second, to complete the calibration, one of the coils (#4) was calibrated in an absolute sense. This was done with a surface calibration. The transmitter coil was laid out on the ground surface, and the desired receiver coil was laid out so the two coil axes were parallel and so that the centers of the two coils were on a line perpendicular to both coils (broadside). The transmitter coil was excited at the same frequency and current drive level that was used to collect the data, while the receiver coil was placed at distances of 15, 20, 25, and 30 m from the transmitter. Magnitude and phase data were collected at each location.

The third and final step in the calibration process consists of plotting the data for coil #4 (magnitude and phase of the coil output voltage/transmitter coil current) versus distance on a log-log scale. When the calibration has been done correctly, the magnitude data will plot as a straight line with a particular slope, m. For example, in the free space case, $m = -3$, and the magnetic field varies as r^{-3}. These data are then fitted to a half-space or layered model of the earth using a well-verified EM modeling code such as EM1D (Ki Ha Lee, LBNL) and adjusting the model conductivities. When the slopes from the data plots and the half space model match, then EM1D and the calibration data for coil #4 can be used to calculate the appropriate calibrations for coil #4. The calibration for coil #4 and the relative calibrations for coils 1, 2, and 3 can then be used to reduce the survey data. The detailed derivation of this calibration procedure is not included here for lack of space.

We have also done some 3-dimensional forward modeling for the purpose of comparison to the measured data using our new code FDFD (Champagne *et al.*, 1999) which is described in more detail in an accompanying paper. The modeling space we have used in shown in plan and sectional views in Figures 3 and 4. As in Figure 1, the North and West survey lines are shown.

We present plots of normalized magnetic field magnitude and phase versus transmitter depth. Both the experimental and the model data are shown. We begin by showing Figure 5 which is a plot of normalized vertical magnetic field magnitude versus transmitter depth for the North profile for a receiver located at 20 m. The solid curve which extends to a depth of 120 m is the experimental plot. The dips in the experimental curve and the associated spikes at approximately 56, 77, 94, and 111 m are caused by the transmitter coil passing by metal centralizers in the transmitter well, and the data in the immediate region are invalid, due to screening effects. The corresponding phase plot is shown in Figure 6.

Looking farther out along the North profile, Figure 7 shows the normalized vertical magnetic field magnitudes for the 40 m case. Figure 8 shows the corresponding phase plots.

The match in shape between the experimental and model plots of magnitude is good; however, there is an offset in magnitude between the experimental and model data in which the model data are about 50% higher than the experimental data. The phase data for the 20 m and 40 m cases show the correct overall shape, but the phase transitions at ± 180 degrees are offset between the experimental and model data.

The agreement between the experimental and model data becomes worse as one moves away from the transmitter well. Comparisons between the experimental and model data at 60 m, 80 m, and 100 m (not shown) show unphysical behavior (a significant dip followed by a slight increase) in the experimental plots when the transmitter depth is about 100 to 120 m.

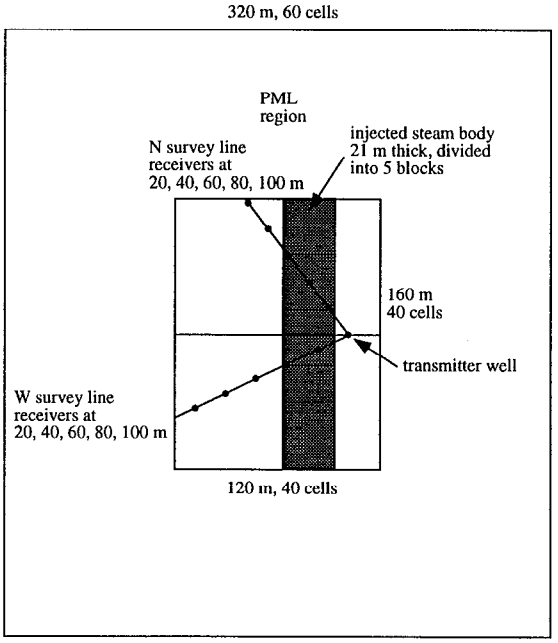

Figure 3: Plan view of problem space and PML regions for FDFD forward modeling.

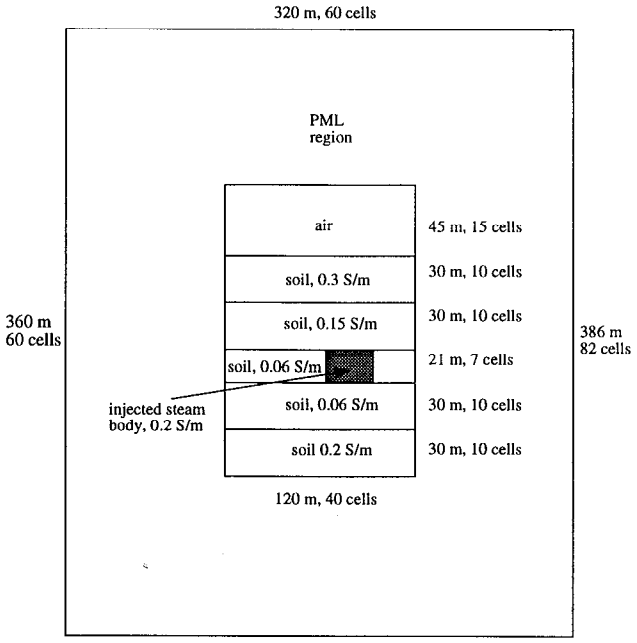

Figure 4: Sectional view of problem space and PML regions for FDFD forward modeling.

The offsets in the magnitude and phase plots could easily be caused by errors in the assumed earth model for the computer code calculations or by errors in the coil calibrations, but the sort of apparently unphysical behavior that is observed in the data for 60 m, 80 m, and 100 m receiver locations probably has another source. The most likely cause, in our opinion, is related to the presence of metallic pipes on the surface (part of the plumbing for steam injection) near or crossing the survey lines which create scattered fields, thereby contaminating the data.

Results for the West profile are similar to that for the North. There is good agreement between the shapes of experimental and model curves for receivers close to the transmitter well, but the agreement again deteriorates as the receiver moves away from the transmitter location.

Results for the radial magnetic field components are not presented here for lack of space. Suffice it to say that the agreement between the experimental and model data plots is as good or better than for the vertical components. In addition the sort of apparently nonphysical behavior that one sees in the vertical magnetic fields is much less obvious in the radial components.

5 Conclusions

The experimental data collected at Lost Hills show reasonable agreement with 3-dimensional forward EM modeling using our new code FDFD (Champagne *et al.*, 1999), especially when the receiver coil is not too far from the transmitter well. At receiver distances greater than about 60 m, the experimental data for the vertical component show apparently unphysical behavior, which we attribute to the presence of metallic conductors (pipes) on the ground surface in the

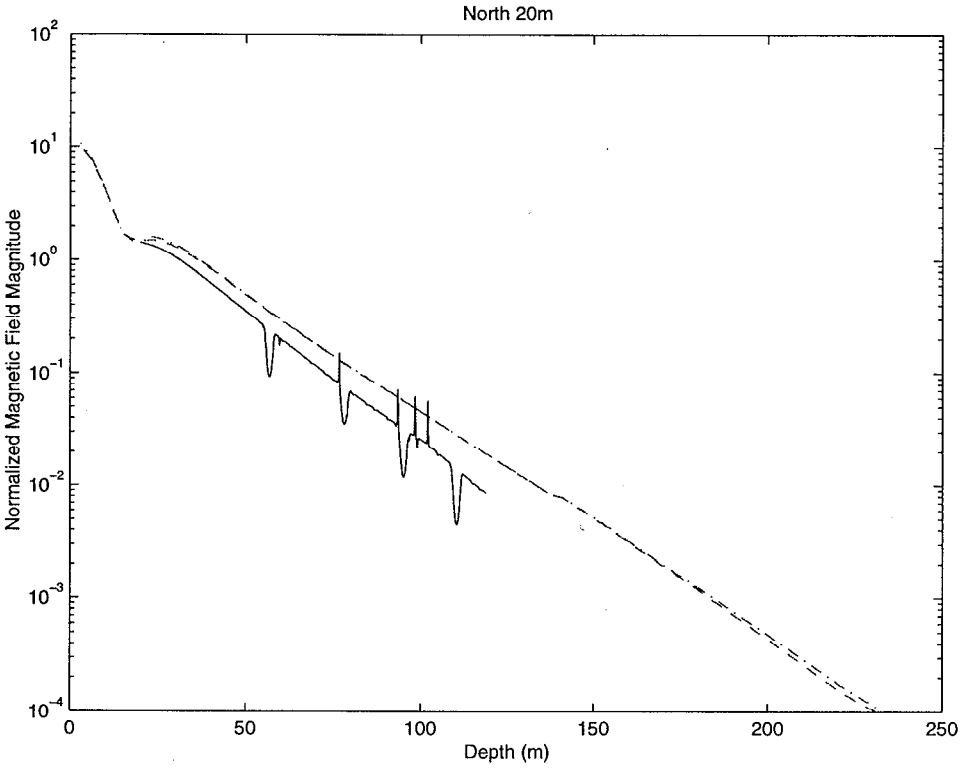

Figure 5: Normalized vertical field magnitude for North survey at 20 m

oil field. This effect seems to be more pronounced in the vertical field components than in the radial components. These results could have been anticipated since induced currents flowing in such horizontal metallic conductors will generate magnetic fields whose polarization is primarily vertical.

Our results confirm that the EMIT technique is viable for steam flood imaging at the Lost Hills site. Future work will concentrate on development of reliable qualitative imaging and quantitative inversion of EMIT data.

Acknowledgments

This work was performed under the auspices of the U.S. Department of Energy by the Lawrence Livermore National Laboratory under contract No. W-7405-ENG-48 and supported specifically by the Environmental Management Science Program of the Office of Environmental Management and the Office of Energy Research.

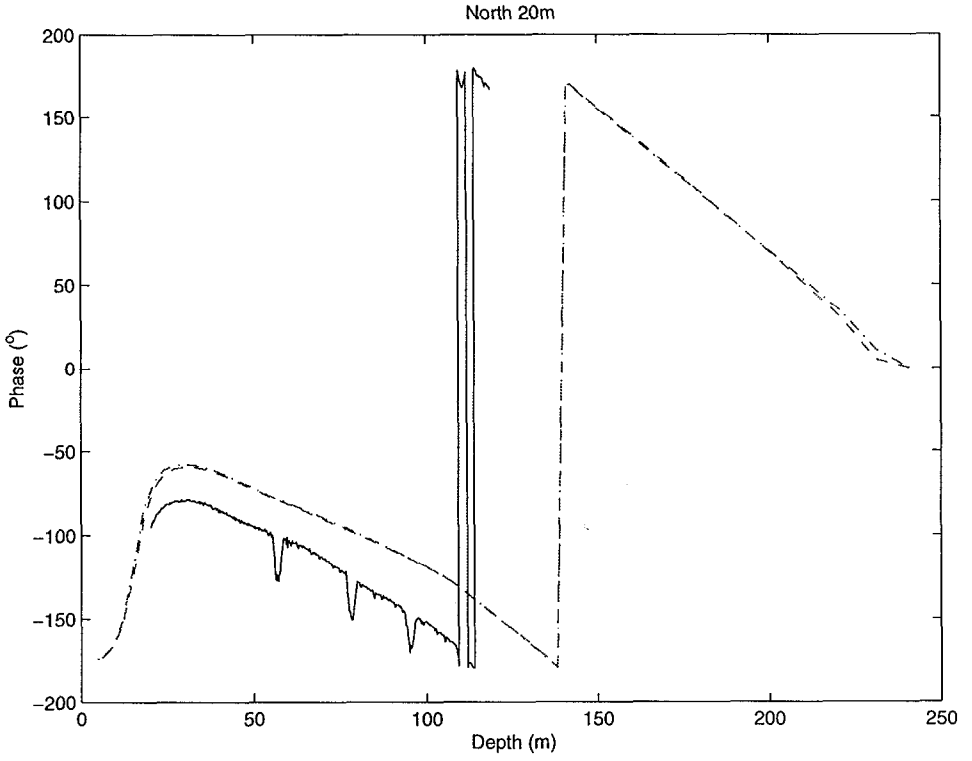

Figure 6: Phase of vertical field for North survey at 20 m

References

Alumbaugh, D. L, and H. F. Morrison, 1995a, Monitoring subsurface changes over time with cross-well electromagnetic tomography, *Geophysical Prospecting* **43**, 873–902.

Alumbaugh, D. L., and H. F. Morrison, 1995b, Theoretical and practical considerations for crosswell electromagnetic tomography assuming cylindrical geometry, *Geophysics* **60**, 846–870.

Berryman, J. G., 1997, Challenges for computational physics in underground imaging of electrically conducting contaminant plumes, invited talk P2.03 in special session on Geological Phenomena at the *International Conference on Computational Physics*, American Physical Society, Division of Computational Physics, Santa Cruz, California, August 25–29, 1997.

Berryman, J. G., 1998, Underground imaging of electrically conducting plumes, invited talk at the International Advanced Studies Institute, First International Symposium on *Detection and Analysis of Subsurface Objects and Phenomena*, Naval Postgraduate School, Monterey, California, October 19–23, 1998.

Berryman, J. G., and R. V. Kohn, 1990, Variational constraints for electrical impedance tomography, *Phys. Rev. Lett. 65*, 325-328.

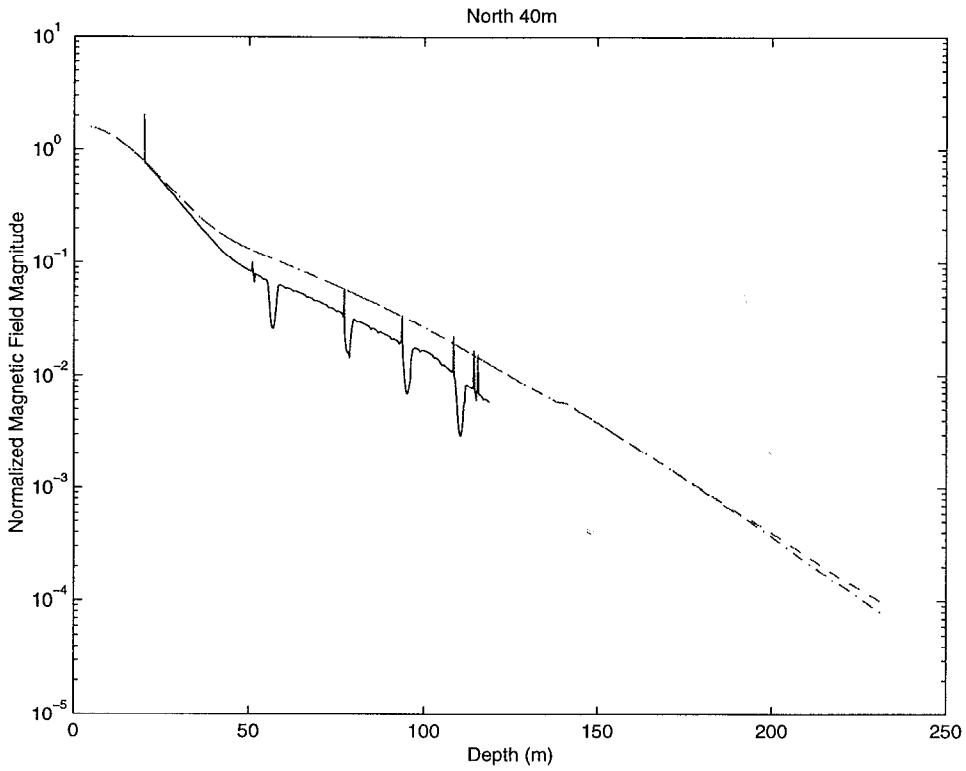

Figure 7: Normalized vertical field magnitude for North survey at 40 m

Borcea, L., 1996, *Direct and Inverse Problems for Transport in High Contrast Media*, Ph.D. thesis, Stanford University, May, 1996.

Borcea, L., J. G. Berryman, and G. C. Papanicolaou, 1996, High contrast impedance tomography, *Inverse Problems* **12**, 835–858.

Champagne, N. J., II, J. G. Berryman, H. M. Buettner, J. B. Grant, and R. M. Sharpe, 1999, A finite-difference Fourier-domain code for electromagnetic induction tomography, SAGEEP, Oakland Marriott Center, Oakland, California, March 14–18, 1999.

Daily, W. D., A. Ramirez, D. LaBrecque, and J. Nitao, 1992, Electrical resistivity tomography of vadose water movement, *Water Resources Res.* **28**, 1429–1442.

Newmark, R. L., and M. J. Wilt, 1992, Monitoring underground steam injection using geophysical logs, in *Dynamic Underground Stripping Demonstration Project — Interim Engineering Report*, edited by R. L. Newmark, LLNL UCRL-ID-110064, April, 1992, pp. 343–372.

Ramirez, A., W. D. Daily, D. LaBrecque, E. Owen, and D. Chesnut, 1993, Monitoring an underground steam injection process using electrical resistance tomography, *Water Resources Res. 29*, 73–87.

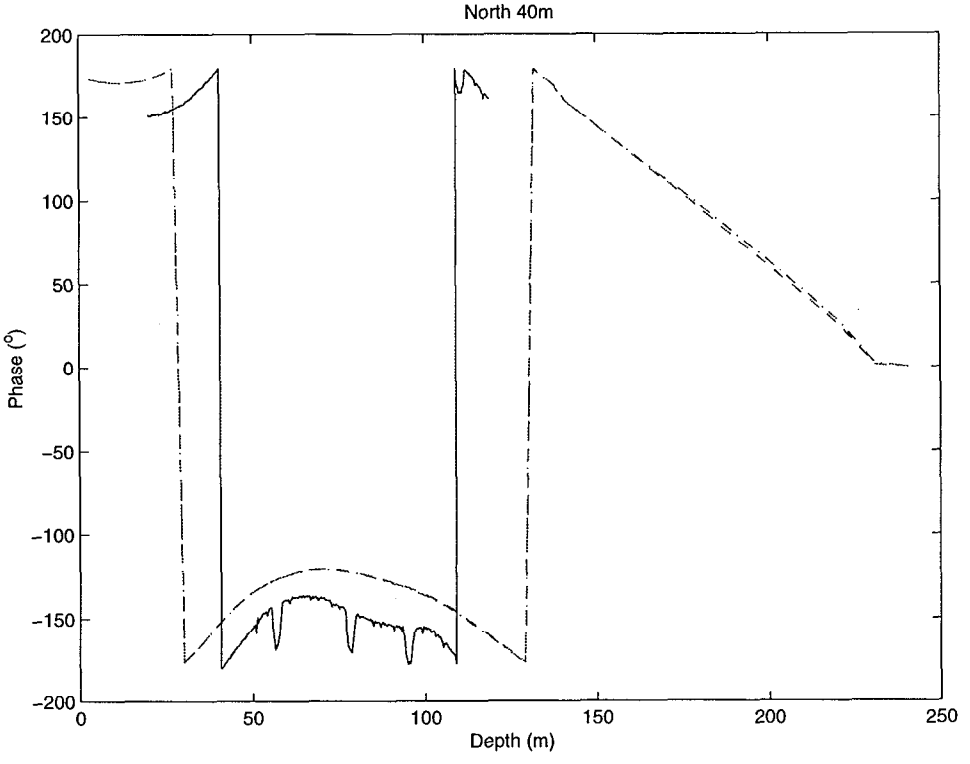

Figure 8: Phase of vertical field for North survey at 40 m

Tseng, H.-W., A. Becker, and M. J. Wilt, 1995, A borehole-to-surface electromagnetic survey, *Society of Exploration Geophysicists Expanded Abstracts*, Proceedings of the International Exposition and Sixty-Fifth Annual Meeting, Houston, Texas, October 8-13, 1995, pp. 246–249.

Wilt, W. J., D. L. Alumbaugh, H. F. Morrison, A. Becker, K. H. Lee, and M. Deszcz-Pan, 1995a, Crosswell electromagnetic tomography: System design considerations and field results, *Geophysics* **60**, 871–885.

Wilt, M., H. F. Morrison, A. Becker, H.-W. Tseng, K. H. Lee, C. Torres-Verdin, and D. Alumbaugh, 1995b, Crosshole electromagnetic tomography: A new technology for oil field characterication, *The Leading Edge* **14**, March, 1995, pp. 173–177.

Wilt, M. J., and C. Schenkel, 1992, Cross-borehole electromagnetic induction at the Dynamic Underground Stripping clean site, in *Dynamic Underground Stripping Demonstration Project - Interim Engineering Report*, edited by R. L. Newmark, LLNL UCRL-ID-110064, April, 1992, pp. 407–425.

Wilt, M. J., C. Schenkel, M. Wratcher, I. Lambert, C. Torres-Verdin, and H.-W. Tseng, 1996, Crosshole EM for oil field characterizationa and EOR monitoring: Field examples from Lost Hills, California, LLNL UCRL-ID-123893, July 16, 1996.